Rho-dependent control of anillin behavior during cytokinesis

Gilles R.X. Hickson and Patrick H. O'Farrell

Department of Biochemistry and Biophysics, University of California, San Francisco, San Francisco, CA 94158

Anillin is a conserved protein required for cytokinesis but its molecular function is unclear. Anillin accumulation at the cleavage furrow is Rho guanine nucleotide exchange factor (GEF)^{Pbl}–dependent but may also be mediated by known anillin interactions with F-actin and myosin II, which are under RhoGEF^{Pbl}-dependent control themselves. Microscopy of *Drosophila melanogaster* S2 cells reveal here that although myosin II and F-actin do contribute, equatorial anillin localization persists in their absence. Using latrunculin A, the inhibitor of F-actin assembly, we uncovered a separate RhoGEF^{Pbl}-dependent pathway that, at the normal time of furrowing, allows stable filamentous structures containing anillin, Rho1, and septins to form directly at the equatorial plasma membrane. These structures associate with microtubule (MT) ends and can still form after MT depolymerization, although they are delocalized under such conditions. Thus, a novel RhoGEF^{Pbl}-dependent input promotes the simultaneous association of anillin with the plasma membrane, septins, and MTs, independently of F-actin. We propose that such interactions occur dynamically and transiently to promote furrow stability.

Introduction

Cytokinesis follows a complex spatiotemporal program initiated at anaphase onset. It proceeds through several steps, including cleavage furrow formation, ingression, midbody formation, and abscission (Glotzer, 2005; Eggert et al., 2006). Many conserved proteins, including regulators of F-actin and myosin II, localize to the cytokinetic apparatus and are required for cytokinesis, but how they localize there and function together remains unclear. A conserved Rho guanine nucleotide exchange factor (GEF), encoded by *pebble* in *Drosophila melanogaster* (Prokopenko et al., 1999), guides furrowing, in part through stimulation of F-actin assembly via the formin Diaphanous (Dia; Castrillon and Wasserman, 1994) as well as through activation of Rho kinase (Rok) and myosin II (Dean et al., 2005; Matsumura, 2005; Dean and Spudich, 2006; Hickson et al., 2006).

Another conserved furrow component is anillin, a putative scaffolding protein that can bind F-actin, myosin II, and septins, although the significance of these interactions is unclear (Field and Alberts, 1995; Oegema et al., 2000; Paoletti and Chang, 2005; Straight et al., 2005). Anillin localizes to the furrow early, but its essential requirement appears to be for furrow stability and midbody formation later in cytokinesis (Somma et al., 2002; Echard et al., 2004; Straight et al., 2005; Zhao and Fang, 2005). It is not understood how anillin localizes to the furrow, although it appears to require RhoGEF^{Pbl} (Prokopenko et al., 1999) and can occur independently of myosin II function (Straight et al., 2003, 2005).

Using high-resolution microscopic assays, we have analyzed the behavior of anillin at the time of cytokinesis. We find that a unique and previously unrecognized Rho-dependent input can, independently of F-actin, promote the association of anillin with septins, the plasma membrane, and microtubules (MTs), thus providing insight into how anillin operates during cytokinesis.

Results and discussion

We generated *D. melanogaster* S2 cell lines expressing anillin-GFP. The anillin-GFP fusion rescued loss of endogenous anillin (Fig. S1, available at http://www.jcb.org/cgi/content/full/jcb.200709005/DC1) and its localization paralleled that of endogenous anillin. In interphase it was nuclear, at metaphase it was uniformly cortical, and in anaphase it accumulated at the equator while being lost from the poles (Fig. 1, A and A′; and Video 1, available at http://www.jcb.org/cgi/content/full/jcb.200709005/DC1; Field and Alberts, 1995; Echard et al., 2004). In some highly expressing cells, nuclear anillin-GFP formed filaments not ordinarily seen with anillin immunofluorescence

Correspondence to Gilles Hickson: gilles.hickson@ucsf.edu

Abbreviations used in this paper: Dia, Diaphanous; GEF, guanine nucleotide exchange factor; LatA, Latrunculin A; MRLC, myosin regulatory light chain; MT, microtubule; Rok, Rho kinase.

The online version of this paper contains supplemental material.

The Journal of Cell Biology, Vol. 180, No. 2, January 28, 2008 285–294
http://www.jcb.org/cgi/doi/10.1083/jcb.200709005

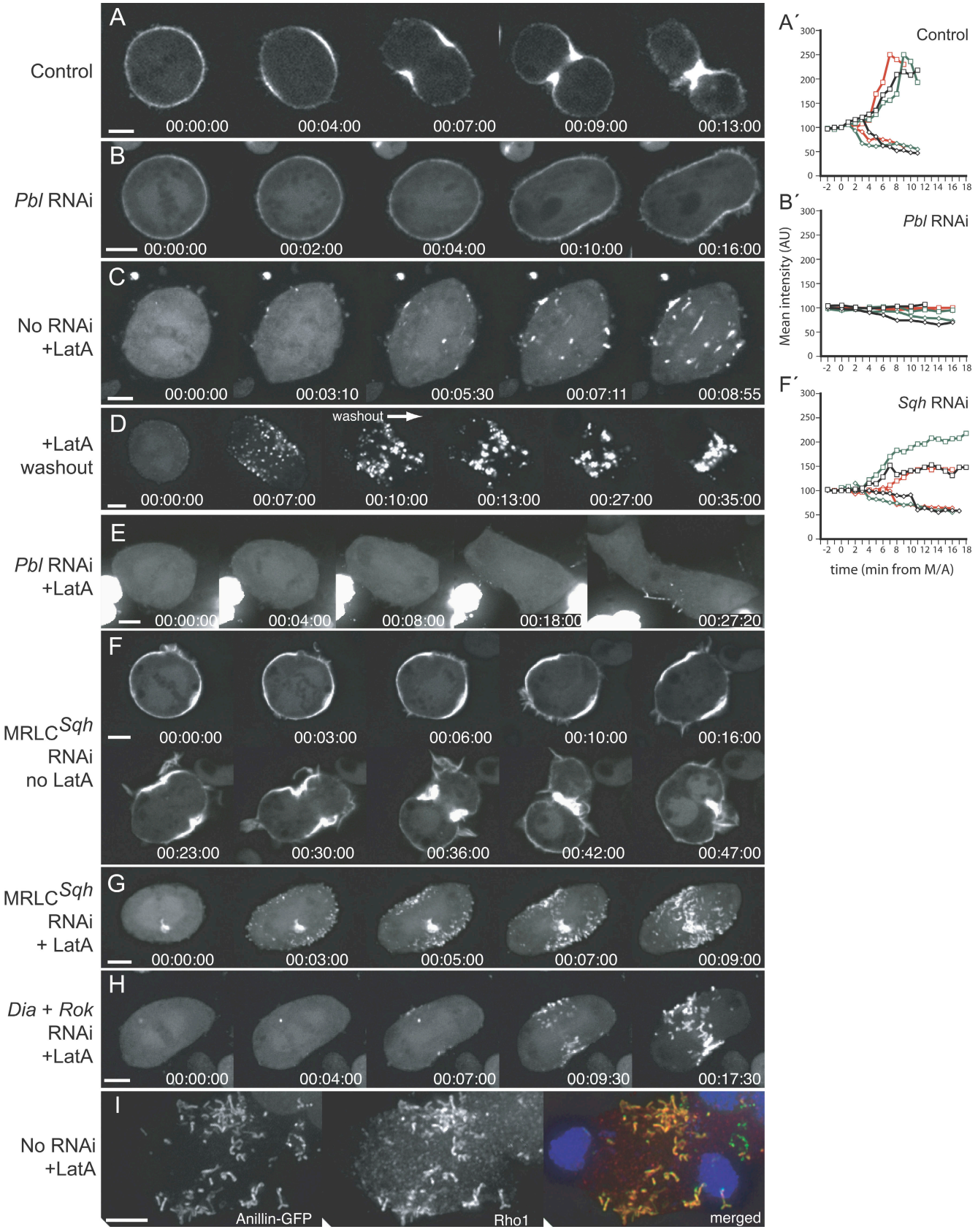

Figure 1. **RhoGEF^{Pbl} controls anillin-GFP localization during anaphase via F-actin– and myosin II–dependent and –independent mechanisms.** (A–H) Frames from time-lapse sequences of anillin-GFP cells progressing through anaphase/telophase (single Z sections, except for D, G, and H, which are projections of five sections). (A) A control cell showing the normal redistribution of anillin-GFP (see Video 1, available at http://www.jcb.org/cgi/content/full/jcb.200709005/DC1). (B) A cell after 3 d of RhoGEF^{Pbl} RNAi (see Video 2). (C) A cell after 1-μg/ml LatA treatment (surface Z section; see Video 3).

(unpublished data), but these disassembled upon nuclear envelope breakdown and the overexpression had no appreciable effect on the progress or success of cytokinesis.

Equatorial localization of anillin-GFP during anaphase occurs via multiple RhoGEF^{Pbl}-dependent mechanisms

We tested whether RhoGEF^{Pbl} contributed to anillin localization during cytokinesis. After 3 d of RhoGEF^{Pbl} RNAi or *Rho1* RNAi (unpublished data), anillin-GFP localized to the cortex in metaphase but did not relocalize to the equator during anaphase (Fig. 1, B and B′; and Video 2, available at http://www.jcb.org/cgi/content/full/jcb.200709005/DC1), indicating a requirement for RhoGEF^{Pbl} that is consistent with prior analysis of fixed RhoGEF^{Pbl} mutant embryos (Prokopenko et al., 1999). Because anillin can bind F-actin (Field and Alberts, 1995) and phosphorylated myosin regulatory light chain (MRLC; Straight et al., 2005), RhoGEF^{Pbl} might regulate anillin indirectly through its control of F-actin and myosin II.

We used latrunculin A (LatA) to test whether F-actin was required for anillin-GFP localization. A 30–60-min incubation of 1 µg/ml LatA abolished cortical anillin-GFP localization in metaphase (Fig. 1 C), indicating an F-actin requirement at this phase. However, when anillin normally relocalizes to the equator (~3–4 min after anaphase onset), anillin-GFP formed punctate structures that became progressively more filamentous over the next few minutes, reaching up to several micrometers in length and having a thickness of ~0.3 µm (Fig. 1 C and Video 3, available at http://www.jcb.org/cgi/content/full/jcb.200709005/DC1). These linear anillin-containing structures contained barely detectable levels of F-actin (Fig. S2) and formed specifically at the plasma membrane and preferentially at the equator, although subsequent lateral movement often led to a more random distribution (Fig. 1 C and Video 3). Thus, anillin responds to spatiotemporal cytokinetic cues even after major disruption of the F-actin cytoskeleton. A substantial (albeit incomplete) reacquisition of cortical phalloidin staining was observed in cells fixed after washing out the drug for a few minutes (unpublished data). In live cells, LatA washout immediately after formation of the anillin structures allowed the preformed structures to migrate from a broad to a compact equatorial zone as the cells attempted to complete cytokinesis (Fig. 1 D and Video 4). This movement indicates that an F-actin–dependent process can contribute to the equatorial focusing of anillin.

We tested the influence of RhoGEF^{Pbl} on anillin behavior in LatA. After RNAi of RhoGEF^{Pbl} (Fig. 1 E) or *Rho1* (not depicted), anillin-GFP remained cytoplasmic through anaphase. Thus RhoGEF^{Pbl} and Rho1 are required for anaphase anillin behavior, whether the cortex is intact or disrupted by LatA treatment.

We tested whether myosin II impacted anillin-GFP localization. Compared with controls (Fig. 1, A and A′), RNAi of the gene encoding MRLC *spaghetti squash* (MRLC^{Sqh}; Karess et al., 1991) inhibited cell elongation during anaphase (Hickson et al., 2006), slowed furrow formation, and delayed and diminished the equatorial localization of anillin-GFP (Fig. 1, F and F′; and Video 5, available at http://www.jcb.org/cgi/content/full/jcb.200709005/DC1). However, unlike after RhoGEF^{Pbl} RNAi, equatorial accumulation of anillin-GFP was not altogether blocked. It was still recruited but in a broad zone (Fig. 1 F). Furthermore, in the presence of LatA, MRLC^{Sqh} RNAi did not affect the formation of the anillin-GFP structures (Fig. 1 G). We conclude that myosin II contributes to the equatorial focusing of anillin when the F-actin cortex is unperturbed but that myosin II is dispensable for anillin behavior in LatA.

Collectively, these data suggest that multiple RhoGEF^{Pbl}-dependent inputs control anillin localization. The slowed equatorial accumulation of anillin when myosin II function was impaired indicates a myosin II–dependent input. That reassembly of the cortical F-actin network (after washout of LatA) allowed preformed anillin structures to move toward the cell equator indicates an F-actin–dependent input. This is consistent with the concerted actions of myosin II and F-actin driving cortical flow, as observed in other cells (Koppel et al., 1982; Cao and Wang, 1990; Wang et al., 1994; DeBiasio et al., 1996; Fishkind et al., 1996), and is reminiscent of the coalescence of cortical nodes during contractile ring assembly in *Schizosaccharomyces pombe* (Wu et al., 2006). However, the F-actin– and myosin II–independent behavior of anillin in LatA indicates an additional RhoGEF^{Pbl}-dependent input. We tested possible involvement of Dia or Rok, the Rho effectors responsible for cytokinetic F-actin assembly and myosin II activation, respectively. Neither *Dia* nor *Rok* RNAi, alone or combined (Fig. 1 H and Fig. S3, available at http://www.jcb.org/cgi/content/full/jcb.200709005/DC1), prevented formation of the anillin structures in LatA, indicating that they too were dispensable. Thus, RhoGEF^{Pbl} can control anillin behavior in anaphase via a previously unrecognized route. Immunofluorescence analysis revealed extensive colocalization between endogenous Rho1 and anillin-GFP in LatA, indicating that Rho1 was itself a component of these structures (Fig. 1 I). Although other Rho effectors could be involved, our findings are consistent with prior indications that Rho1 and anillin may directly interact (Suzuki et al., 2005).

Equatorial accumulation of myosin II during anaphase can occur independently of F-actin and anillin, but stable furrow positioning requires anillin

We examined myosin II localization (Fig. 2 A), as it can bind anillin and is controlled by RhoGEF^{Pbl}. As previously reported

(D) The same as C but the LatA was washed out at 10 min, soon after the formation of anillin-GFP structures (see Video 4). (E) A cell after 3 d of RhoGEF^{Pbl} RNAi and LatA combined. (F) A cell after 3 d of *MRLC^{Sqh}* RNAi (see Video 5). (G) A cell after MRLC^{Sqh} RNAi and LatA combined. (H) A cell after 4 d of Dia and Rok RNAi and LatA treatment combined. (I) A LatA-treated anillin-GFP cell fixed during anaphase/telophase and labeled with a Rho1 antibody (red in merged; max intensity projection). (A′, B′, and F′) semiquantitative measurements of the mean anillin-GFP intensities at the equator (□) and poles (◊), expressed as arbitrary units (AU) relative to time 0 (metaphase/anaphase [M/A]) in control, Pbl, and Sqh RNAi cells, shown for three cells each (different colors represent different cells). Times are h:min:s from anaphase onset. Bars, 5 µm.

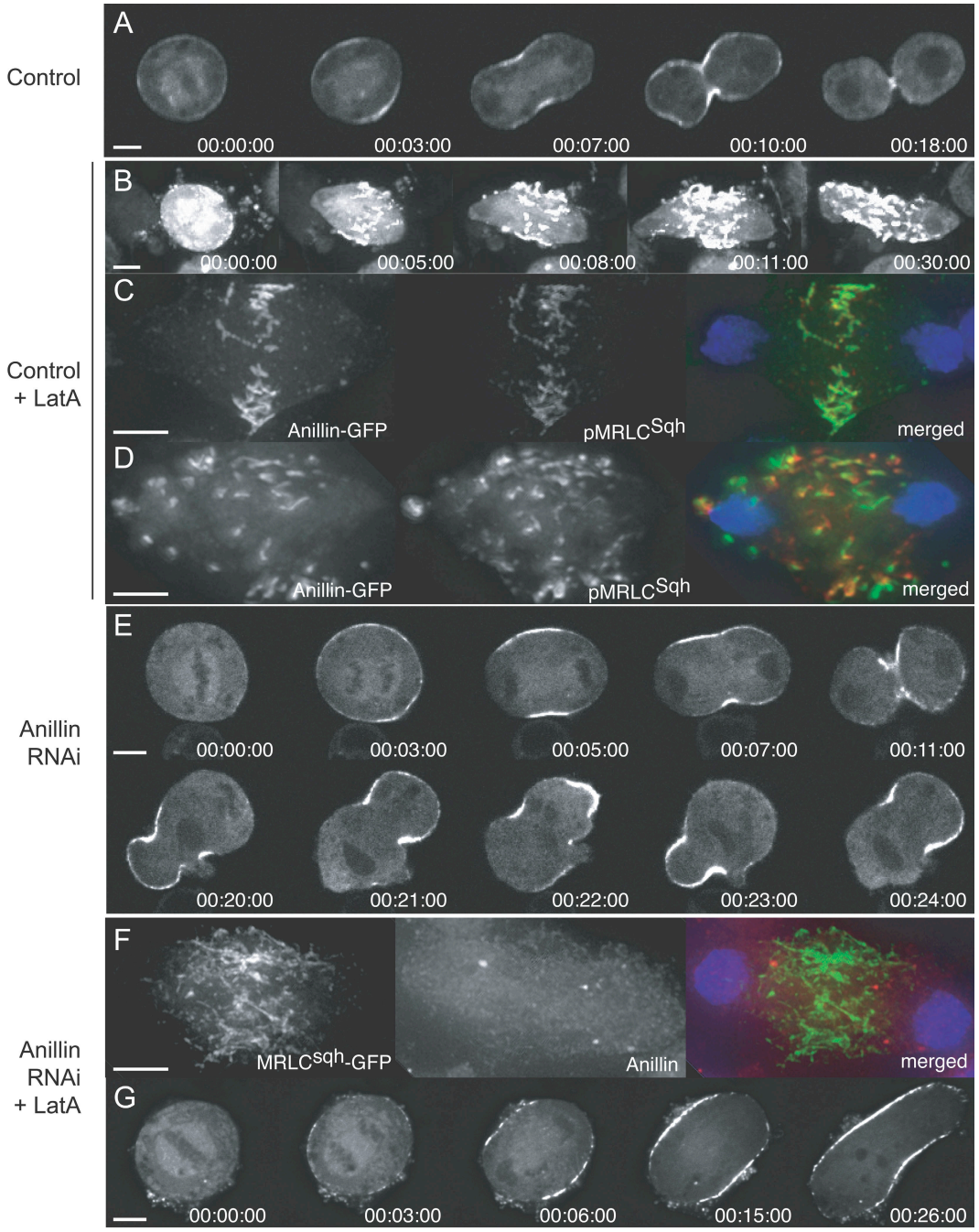

Figure 2. **Myosin II localization can occur independently of F-actin and anillin but stable furrow positioning requires anillin.** (A and B) Frames from time-lapse sequences of cells expressing MRLC^{Sqh}-GFP progressing through anaphase. (A) Control cell expressing MRLC^{Sqh}-GFP. (B) Cell treated with LatA. A projection of five 2-μm sections is shown (Video 6, available at http://www.jcb.org/cgi/content/full/jcb.200709005/DC1). (C and D) Cells expressing anillin-GFP (green in merged) fixed during anaphase/telophase in the presence of 1 μg/ml LatA, labeled with a Ser21 phospho-MRLC^{Sqh} antibody (red in merged; maximum intensity projections of multiple 0.25-μm deconvolved sections). (E) Frames from a time-lapse sequence of a MRLC^{Sqh}-GFP cell attempting cytokinesis after 3 d of anillin RNAi (see Video 7). (F) Cell expressing MRLC^{Sqh}-GFP (green in merged), fixed during anaphase in the presence of LatA after anillin RNAi and labeled with an anillin antibody (red in merged; maximum intensity projection of multiple 0.25-μm deconvolved sections). (G) Frames from a time-lapse sequence of a cell expressing MRLC^{Sqh}-GFP attempting cytokinesis after 3 d of anillin RNAi and in the presence of LatA (projection of five 2-μm sections; see Video 8). Times are h:min:s from anaphase onset. Bars, 5 μm.

(Dean et al., 2005), MRLC^{Sqh}-GFP was able to localize to the equatorial membrane independently of F-actin, and in doing so formed filamentous structures resembling those observed with anillin-GFP (Fig. 2 B and Video 6, available at http://www.jcb.org/cgi/content/full/jcb.200709005/DC1). Indeed, anillin and MRLC^{Sqh} (detected as either MRLC^{Sqh}-GFP or with an antibody to serine 21–phosphorylated pMRLC^{Sqh}) colocalized (Fig. 2 C), although they were often offset as if labeling different regions of the same structures (Fig. 2 D).

We tested the effects of anillin RNAi on MRLC^{Sqh}-GFP localization. MRLC^{Sqh}-GFP recruitment and furrow initiation appeared normal, but within a few minutes of initiation, furrows

became laterally unstable and oscillated back and forth across the cell cortex, parallel to the spindle axis, in repeated cycles, each lasting ~1–2 min and eventually subsiding to yield binucleate cells after ~20 min (Fig. 2 E and Video 7, available at http://www.jcb.org/cgi/content/full/jcb.200709005/DC1). The phenotype was very similar to that reported for anillin RNAi in HeLa cells (Straight et al., 2005; Zhao and Fang, 2005) and represents a requirement for anillin at an earlier stage than previously noted in *D. melanogaster* (Somma et al., 2002; Echard et al., 2004). Thus, a conserved function of anillin is to maintain furrow positioning during ingression. A potential mechanism is proposed in the following paragraph.

In LatA, anillin RNAi did not prevent equatorial MRLC^{Sqh}-GFP recruitment, but instead of appearing as persistent linear structures distorting the cell surface, a more reticular and dynamic structure lacking cell surface protrusions was observed (compare Fig. 2 G and Video 8 [available at http://www.jcb.org/cgi/content/full/jcb.200709005/DC1] with Fig. 2 B and Video 6; and compare Fig. 2 F with Fig. 2 D). Thus myosin II can localize independently of both anillin and F-actin but the filamentous appearance of myosin II in the presence of LatA requires anillin, indicating that anillin can influence myosin II behavior in the absence of F-actin, whereas myosin II appeared capable of influencing anillin behavior only in the presence of F-actin (Fig. 1).

Septins are required for the filamentous structures in LatA and septin recruitment depends on anillin

Septins are multimeric filament-forming proteins that can bind anillin in vitro and function with anillin in vivo (Kinoshita et al., 2002; Field et al., 2005; Maddox et al., 2005, 2007). Using an antibody to the septin Peanut (Neufeld and Rubin, 1994), we found that in nontransfected S2 cells, septin^{Pnut} localized to the cleavage furrow and midbody where it colocalized with anillin (Fig. 3, A and B). Unexpectedly, the septin^{Pnut} antibody also strongly labeled bundles of cytoplasmic ordered cylindrical structures, each ~0.6 µm in diameter and of variable length (up to several micrometers; Fig. 3 B and Fig. S3). These staining patterns could be greatly reduced by septin^{Pnut} RNAi and were thus specific (unpublished data). The cylindrical structures did not appear to be cell cycle regulated, as they were apparent in interphase, mitotic, and postmitotic cells. They also did not colocalize with anillin (Fig. 3, A and B), nor did their stability rely on anillin (unpublished data). Incubation with 1 µg/ml LatA before fixation inevitably led to disassembly of most of these large structures; however, the resulting distribution of septin^{Pnut} depended on the cell cycle phase. In LatA-treated interphase cells, when anillin is nuclear, septin^{Pnut} formed cytoplasmic rings, ~0.6 µm in diameter, which are similar to the Septin2 rings seen in interphase mammalian cells treated with F-actin drugs or in the cell body of unperturbed ruffling cells (Kinoshita et al., 2002; Schmidt and Nichols, 2004). In LatA-treated mitotic cells, septin^{Pnut} was diffusely cytoplasmic (or barely detectable) in early mitosis, whereas in anaphase/telophase, it localized to the same plasma membrane–associated anillin-containing filamentous structures described in Fig. 1, whether marked by anillin-GFP (Fig. 3 C) or antibody staining of endogenous anillin (Fig. S3).

We analyzed anillin behavior after septin^{Pnut} RNAi. Although unable to fully deplete septin^{Pnut}, we found that anillin could localize to the equatorial cortex in regions devoid of detectable septin^{Pnut} (Fig. S3), which is consistent with findings in *Caenorhabditis elegans* (Maddox et al., 2005). Importantly, in septin^{Pnut}-depleted cells, anillin-GFP still localized to the plasma membrane in LatA but no longer appeared filamentous (Fig. 3 D and Video 9, available at http://www.jcb.org/cgi/content/full/jcb.200709005/DC1), indicating that septin^{Pnut} is essential for the filamentous nature of the structures and that Rho1 can promote the association of anillin with the plasma membrane independently of septin^{Pnut}. However, in this case the plasma membrane to which anillin-GFP localized subsequently exhibited unusual behavior. It was internalized in large vesicular structures, apparently in association with midzone MTs (Fig. S3 and Video 9). Although we do not understand this phenomenon, it may be related to events induced by point mutations in the septin-interacting region of anillin that give rise to abnormal vesicularized plasma membranes during *D. melanogaster* cellularization (Field et al., 2005).

We tested the effects of anillin RNAi on the localization of septin^{Pnut}. Using Dia as a furrow marker (Fig. 3 E), 3 d of anillin RNAi prevented the furrow recruitment of septin^{Pnut} (Fig. 3 F). In LatA-treated cells, anillin RNAi did not affect the formation of septin^{Pnut} rings in interphase cells (not depicted), but it greatly reduced the formation of septin^{Pnut}-containing structures during anaphase/telophase (Fig. 3 G). Thus, anillin is required for the furrow recruitment of septin^{Pnut} and for the formation of septin^{Pnut}-containing structures in 1 µg/ml LatA. In contrast, Dia could still localize to the equatorial plasma membrane after combined anillin RNAi and LatA treatment (Fig. 3 G), indicating that it can localize independently of both anillin and F-actin. Thus, although Dia partially colocalized with anillin in LatA (Fig. S3), this likely reflected independent targeting to the same location rather than an association between anillin and Dia.

Our data argue that Rho1, anillin, septins, and the plasma membrane participate independently of F-actin in the formation of a complex. However, anillin, septins and F-actin can also form a different complex in vitro, independently of Rho (Kinoshita et al., 2002). Perhaps two such complexes dynamically interchange in vivo.

A potential role for anillin in anchoring the cleavage furrow to midzone MTs

We tested the involvement of MTs in anillin behavior in LatA. Overnight incubation with 25 µM colchicine effectively depolymerized all MTs in mitotic cells and promoted mitotic arrest, as expected (unpublished data). Using Mad2 RNAi to bypass the arrest (Logarinho et al., 2004), we observed anillin-GFP during mitotic exit in the absence of MTs and in the presence of LatA (Fig. 4 A). Under such conditions, anillin-GFP formed filamentous structures very similar to those formed when MTs were present, indicating that MTs were dispensable for their formation. However, the structures appeared uniformly around the plasma membrane rather than restricted to the equatorial region (Fig. 4 A), which is consistent with the role MTs play in the spatial control of Rho activation (Somers and Saint, 2003;

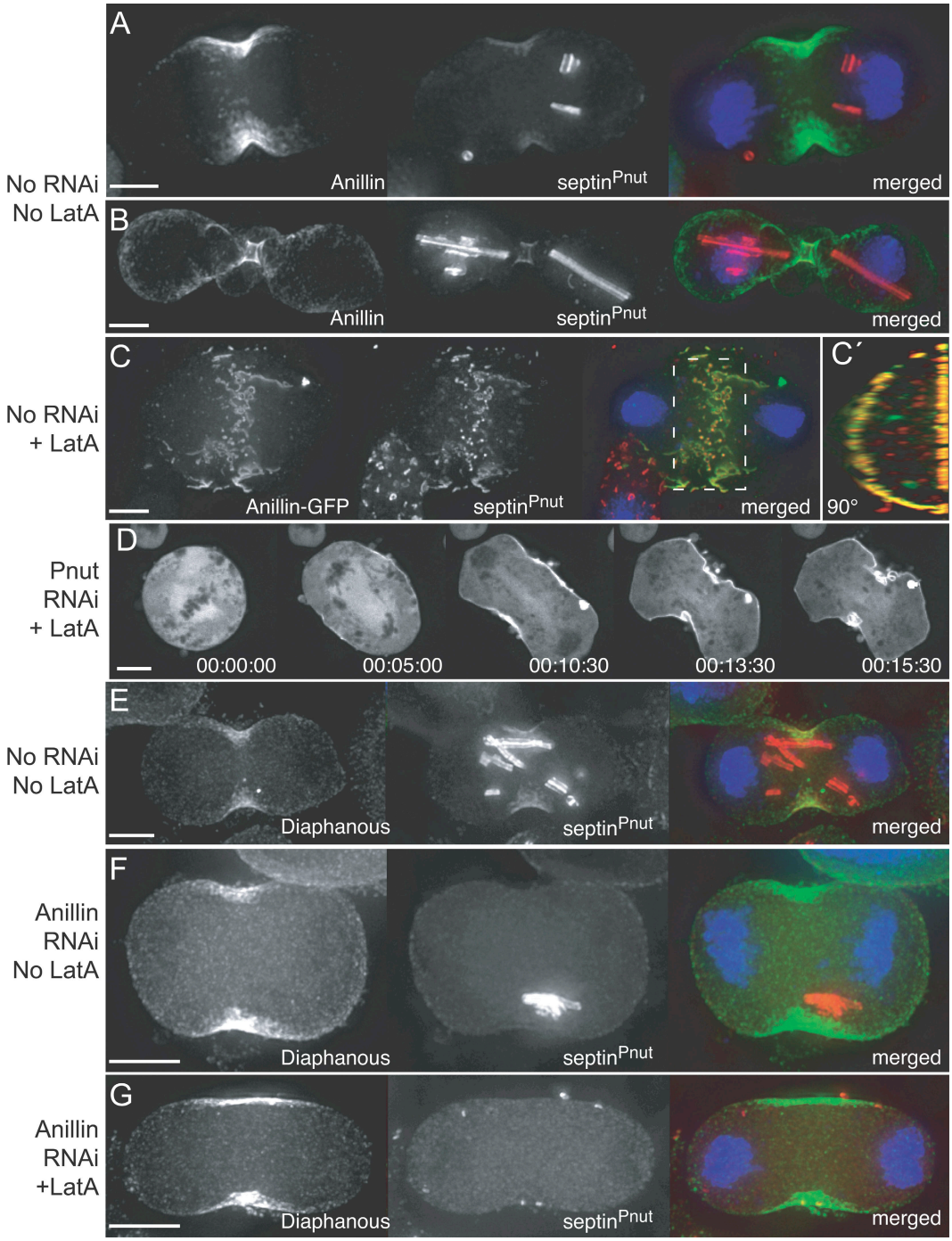

Figure 3. **Anillin recruits septin to the cleavage furrow and to filamentous structures in LatA.** (A–C) Nontransfected (A and B) and anillin-GFP–expressing (C) S2 cells fixed during anaphase/telophase and labeled with antibodies to septin^{Pnut} (middle; red in merged) and anillin (A and B, left; green in merged) and the DNA stain HOECHST (blue in merged; maximum intensity projections of deconvolved 0.25-µm sections). C′ is a 90° rotation about the y axis of the projected stack within the boxed region in C. (D) Time-lapse sequence of a cell expressing anillin-GFP attempting cytokinesis in the presence of LatA after 6 d of septin^{Pnut} RNAi. (E–G) Nontransfected S2 cells fixed during anaphase/telophase and labeled with antibodies to septin^{Pnut} (middle; red in merged) and Dia (left; green in merged) and the DNA stain HOECHST (blue in merged; maximum intensity projections of deconvolved 0.25-µm sections). (E) Control cell. (F) Cell after 3 d of anillin RNAi. (G) Cell after 3 d of anillin RNAi and LatA treatment combined. Bars, 5 µm.

Bement et al., 2005; Yuce et al., 2005; Piekny et al., 2005; Kamijo et al., 2006).

Shown by immunofluorescence, the LatA-induced anillin structures localized to the ends of nonoverlapping astral MTs directed toward the equator (Fig. 4 B, endogenous anillin). Live imaging of cells coexpressing cherry-tubulin and anillin-GFP revealed bundles of MTs associating with the filamentous anillin-GFP structures as they formed (Fig. 4, C and D; and Video 10, available at http://www.jcb.org/cgi/content/full/jcb.200709005/DC1). Colocalization between anillin-GFP structures and MT ends persisted over many minutes, even after considerable lateral movement at the membrane. Thus, although

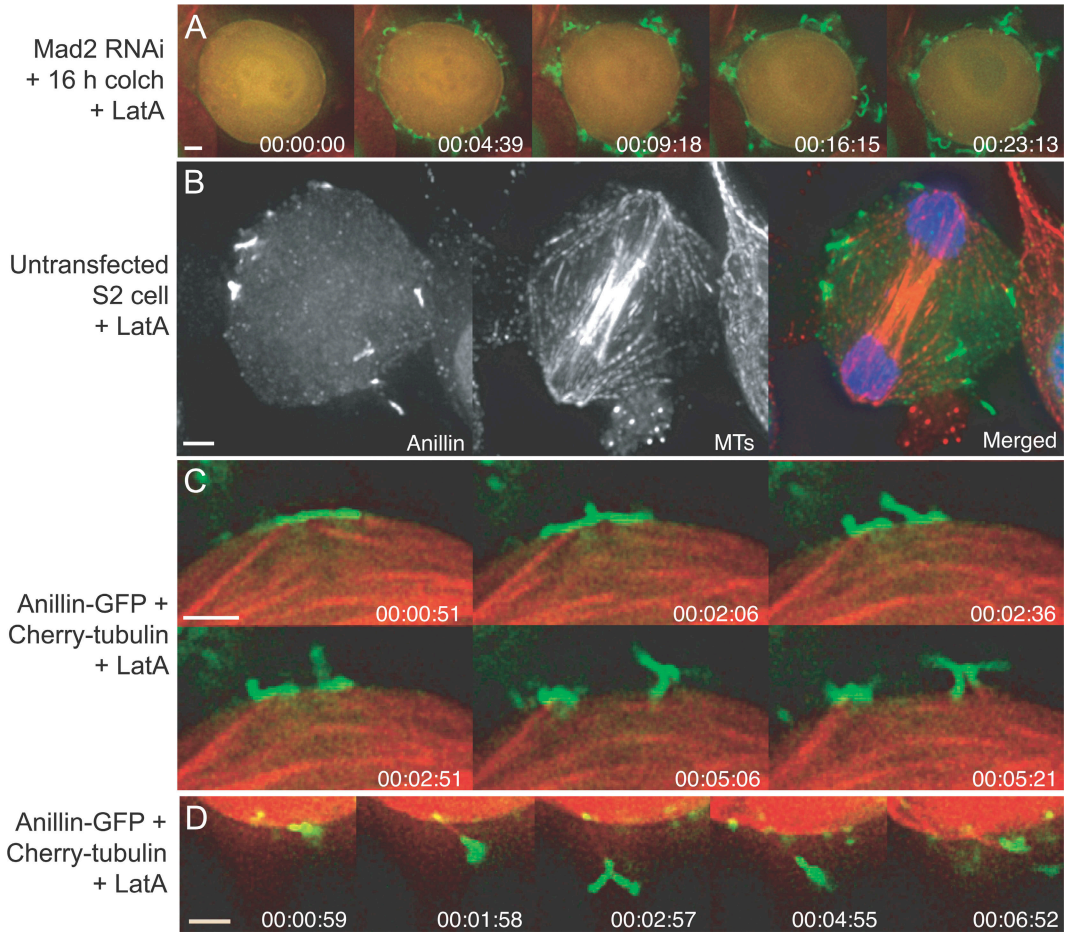

Figure 4. **Anillin-containing structures in LatA form independently of MTs but associate with MT ends at the plasma membrane.** (A) Time-lapse sequence of a cell expressing anillin-GFP and mcherry-tubulin exiting mitosis in the presence of colchicine (16 h) and LatA (1 h) after 3 d of Mad2 RNAi (max intensity projections of deconvolved 2-µm sections). (B) A nontransfected S2 cell treated with LatA and labeled with antibodies to anillin (green in merged) and α-tubulin (red in merged; max intensity projection of multiple deconvolved 0.25-µm sections). (C and D) Frames from time-lapse sequences of cells coexpressing anillin-GFP and mcherry-tubulin progressing through anaphase in the presence of 1 µg/ml LatA (see Video 10, available at http://www.jcb.org/cgi/content/full/jcb.200709005/DC1). Although the anillin-GFP channel was contrasted identically for all time points in each time-lapse series, the cherry-tubulin channel in C and D was contrasted for each time point individually to counter the effects of photobleaching. Times are h:min:s from anaphase onset. Bars, 2 µm.

the anillin structures formed independently of MTs, they stably associated with MTs. These findings support prior biochemical evidence for interactions of MTs with both anillin and septins (Sisson et al., 2000) and reveal a potential positive-feedback loop in which MTs directed where Rho1–anillin–septin formed linear structures at the plasma membrane, whereas the structures in turn associated with the MT ends. An MT plus end–binding ability of anillin–septin could explain the furrow instability phenotype elicited by anillin RNAi (Fig. 2). Accordingly, anillin may physically link Rho1 to MT plus ends during furrow ingression, thereby promoting the focusing and retention of active Rho1, thus stabilizing the furrow at the equator (Fig. 5).

Rho-dependent association of anillin with the plasma membrane

These live-cell analyses highlight an unusual behavior of the Rho-dependent anillin-containing structures at the plasma membrane. Initially forming beneath and parallel to the plasma membrane (Fig. 4, C and D), the structures then often lifted on one side to appear perpendicular to the cell surface while remaining anchored at their base by MTs (Fig. 4, C and D; and Video 10). We interpret this reorientation as reflecting avid binding to and subsequent envelopment by the plasma membrane. Although intrinsically stable, the structures exhibited dynamic movement within the plane of the plasma membrane and were capable of sticking to one another, via their ends, giving rise to branched structures (Fig. 5 B, Y shape) that were also capable of breaking apart. Anillin has a pleckstrin homology domain within its septin-interacting region and a membrane-anchoring role of anillin has long been postulated (Field and Alberts, 1995). Our data support such a role and suggest that it is controlled by Rho.

The relationship between events in LatA and the normal events of cytokinesis

Our data highlight the complexity of RhoGEF^{Pbl} signaling and lead to a model in which multiple Rho-dependent inputs synergize to control anillin behavior during cytokinesis (Fig. 5).

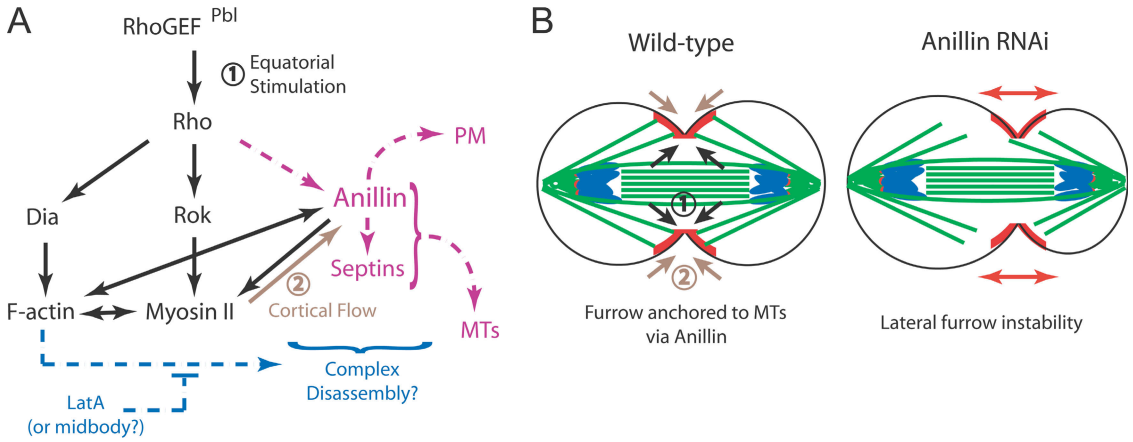

Figure 5. **A model for anillin regulation and function during cytokinesis.** Pathways controlled by RhoGEF^{Pbl}, including well-documented inputs into F-actin and myosin II (black) and a novel, separate input (pink) via anillin and septins (A). Through equatorial stimulation (1), MTs spatially control Rho activation and the independent recruitment of Dia, Rok, and anillin to the equatorial cortex. F-actin and Rok/myosin II contribute to equatorial focusing of anillin (and other cortical components) via cortical flow (2), whereas Rho–anillin–Septin complexes dynamically link contractile elements within the furrow to the plasma membrane (PM) and to MT plus ends, thus preventing the lateral instability of the furrow seen upon anillin RNAi. (B) LatA may stabilize Rho–anillin–Septin complexes by preventing their normal F-actin–dependent disassembly (A, blue). Continued assembly with blocked disassembly gives rise to the filamentous structures in LatA, perhaps mimicking midbody biogenesis that normally accompanies local loss of F-actin at the close of furrowing.

At the appropriate time and location of normal cytokinesis, several proteins, including Rho1, MRLC^{Sqh}, Dia, anillin, and Septin^{Pnut}, localized to the equatorial membrane in the presence of LatA. Of these (and apart from Rho1 itself), anillin and Septin^{Pnut} were uniquely and specifically required for the formation of the linear filamentous structures that we describe. The behaviors of these structures are consistent with prior studies of ordered assemblies of septins and anillin (Oegema et al., 2000; Kinoshita et al., 2002) and of interaction between anillin and MTs (Sisson et al., 2000). Although such structures are not normally seen in furrowing cells, anillin localizes to remarkably similar filamentous structures in the cleavage furrows of HeLa cells arrested with the myosin II inhibitor blebbistatin (see Fig. 5 in Straight et al., 2005).

It seems unlikely that LatA induced the structures we describe through nonspecific aggregation of proteins. Rather, we propose that LatA blocked a normally dynamic disassembly of Rho1–anillin–septin complexes (by blocking an F-actin–dependent process required for the event) and that continued assembly promoted formation of the linear structures (Fig. 5). Because blebbistatin slows F-actin turnover (Guha et al., 2005; Murthy and Wadsworth, 2005), blebbistatin (Straight et al., 2005) and LatA (this study) may have induced filamentous anillin-containing structures via a common mechanism. A dynamic assembly/disassembly cycle involving anillin could promote transient associations between the plasma membrane and elements of the contractile ring and MTs, properties that could contribute to furrow stability and plasticity. Finally, because local loss of F-actin accompanies and may indeed trigger midbody formation (Schroeder, 1972), LatA treatment may have stabilized events in a manner analogous to midbody biogenesis and could therefore be useful in understanding this enigmatic process.

Materials and methods

Molecular biology

The anillin (CG2092-RB) ORF, lacking its stop codon, was amplified using Platinum Taq polymerase (Invitrogen) from clone LD23793 (Gold collection; Drosophila Genomics Resource Center) using primers 5′-CACCATGGACCCGTTTACTCAGCACA-3′ (sense) and 5′-GTGGGTGGTTCCCCAGGC-3′ (antisense) and cloned into the Gateway system pENTR-D-TOPO vector (Invitrogen) according to the manufacturer's protocols. The clone was sequenced and in vitro recombination reactions were performed to transfer the ORF to pMT-WG (inducible *metallothionein* promoter driving C-terminal GFP fusion) and pAc-WG (constitutive *Act05C* promoter) from the *D. melanogaster* Gateway collection (from the T. Murphy laboratory, Carnegie Institute of Washington, Baltimore, MD). The plasmid expressing MRLC^{Sqh}-GFP under the control of the endogenous *Sqh* promoter was described in Rogers et al. (2004); provided by S. Rogers, University of North Carolina, Chapel Hill, NC) and cherry-tubulin in pAc-CW was provided by the R. Vale laboratory (Howard Hughes Medical Institute, University of California, San Francisco, San Francisco, CA).

Cell lines, cell culture, and RNAi

Stable S2 cell lines were generated by cotransfection of plasmids with pCoHygro using Cellfectin reagent followed by selection with hygromycin, all according to the manufacturer's protocols (Invitrogen). Cells were cultured in Schneider's medium supplemented with 10% heat-inactivated FCS and penicillin/streptomycin and passaged every 4–6 d. double-stranded RNAs were synthesized as described in Echard et al. (2004) using Ribomax large-scale transcription kits (Promega) with cDNA templates amplified from genomic whole-fly DNA. Anillin, RhoGEF^{Pbl}, Rok, Dia, and MRLC^{Sqh} double-stranded RNAs were the same as those described in Echard et al. (2004) and Hickson et al. (2006). Others were generated using the following primer pairs: anillin 5′UTR, 5′-CCACCCTGCCAAATACGAC-3′ and 5′-GGGTCCATTGTTGTTGCTGC-3′; anillin 3′UTR, 5′-GGAACCACCCACTGACCCGCT-3′ and 5′-GCGAGTCATCCTAAATTAAATG-3′; and Mad2, 5′-TGCTGGGACTTTAATATGCAGG-3′ and 5′-GCTCATCTTGTAGTTGACCACG-3′. RNAi depletions (performed as in Hickson et al. [2006]), drug treatments, fixations, and imaging were all performed in untreated 96-well glass-bottomed plates (Greiner Bio-One or Whatman). LatA was purchased from EMD and colchicine was purchased from Sigma-Aldrich. LatA (1 μg/ml final concentration) was added for at least 1 h before fixation or imaging. For LatA washout experiments, the LatA-containing medium was removed and replaced three to four times over the course of ∼2 min with fresh medium lacking LatA while the cells were still on the microscope and without pausing the acquisition.

Immunofluorescence

Cells were fixed for 5 min in PBS containing 4% formaldehyde, permeabilized, and blocked for 1 h in PBS containing 0.1% Triton X-100 (PTX) and 5% normal goat serum. Primary antibodies were incubated on the cells overnight at 4°C using the following dilutions: anti-anillin, 1:1,000 (provided by C. Field, Harvard Medical School, Boston, MA; Field and Alberts, 1995); anti-Dia, 1:2,500 (provided by S. Wasserman, University of California, San Diego, La Jolla, CA; Castrillon and Wasserman, 1994); anti–phospho–myosin Light Chain 2 (Ser19, analogous to *D. melanogaster*

MRLC^{Sqh} Ser21) mouse mAb (pMRLC; Cell Signaling Technology), 1:100; anti-tubulin mAb (Sigma-Aldrich), 1:1,000; anti-Peanut (concentrated mAb 4C9H4; Developmental Studies Hybridoma Bank), 1:300; and anti-Rho1 (monoclonal p1D9 supernatant; Developmental Studies Hybridoma Bank), 1:25. Cells were washed several times in PTX before a 1-h incubation with Alexa 488– and 546–conjugated secondary antibodies (1:500; Invitrogen) and HOECHST 33258 (1:500). Cells were washed again in PTX and mounted in Fluoromount-G (SouthernBiotech) before imaging.

Image acquisition and processing

Imaging of fixed cells was performed using a deconvolution system (Deltavision RT; Applied Precision) using an inverted microscope (1×70; Olympus) with a 100× 1.4 NA oil-immersion objective and a cooled charge-coupled device camera (Coolsnap HQ; Photometrics), and Z sections were taken 0.25 µm apart. The resulting datasets were deconvolved using Softworx software (Applied Precision) and maximum intensity projections were saved as TIFF files for export to Photoshop 8.0 (Adobe). Live imaging of cells coexpressing anillin-GFP and cherry-tubulin was also performed using the same system. Images were acquired at room temperature every 20 to 30 s, deconvolved, and exported as mpg or TIFF files for manipulation in Quicktime (Apple) and Photoshop, respectively. Live-cell imaging of cells expressing GFP alone was performed using an inverted microscope (DMIRB; Leica) equipped with 100× 1.3 NA (Plan Fluotar) or 63× 1.4 NA (PlanApo) oil-immersion objectives, a spinning disc (csu 10; Yokogawa), a camera (Orca AG; Hamamatsu), and Volocity v 4 acquisition software (Improvision). Resulting files were exported as Quicktime movies. Frames for the figures were manipulated in Photoshop. Semiquantitative measurements of anillin-GFP fluorescence were performed using Volocity software as follows: for a given cell, the cortex in late metaphase was selected as an object based on a fluorescence intensity value of >0.5–2 standard deviations above the mean intensity for the whole cell. The mean intensity of this object was then used to normalize mean intensity measurements from subsequent time points where regions of the equatorial or polar cortices were similarly selected as objects. Relative differences in mean intensity were calculated from the initial time point in metaphase (set to 100 arbitrary units).

Online supplemental material

Fig. S1 shows rescue of loss of endogenous anillin by expression of anillin-GFP. Fig. S2 shows F-actin staining after treatment with 1 µg/ml LatA. Fig. S3 shows more detailed analysis of the relationship between anillin and septin^{Pnut} or Dia. Video 1 shows a control anillin-GFP–expressing cell progressing through anaphase and cytokinesis and corresponds to Fig. 1 A. Video 2 shows a cell expressing anillin-GFP progressing through anaphase after 3 d of RhoGEF^{Pbl} RNAi and corresponds to Fig. 1 B. Video 3 shows an anillin-GFP–expressing cell progressing through anaphase in the presence of 1 µg/ml LatA and corresponds to Fig. 1 C. Video 4 shows a cell expressing anillin-GFP progressing through anaphase in the presence of 1 µg/ml LatA to allow anillin filament formation, after which the LatA was immediately washed out (over 2 min starting at 10 min from anaphase onset). This corresponds to Fig. 1 D. Video 5 shows a cell expressing anillin-GFP progressing through anaphase after 4 d of MRLC^{Sqh} RNAi and corresponds to Fig. 1 F. Video 6 shows a cell expressing MRLC^{Sqh}-GFP progressing through mitosis in the presence of 1 µg/ml LatA and corresponds to Fig. 2 B. Video 7 shows a cell expressing MRLC^{Sqh}-GFP progressing through anaphase and cytokinesis in the absence of LatA after 3 d of anillin RNAi. This corresponds to Fig. 2 E. Video 8 shows a cell expressing MRLC^{Sqh}-GFP progressing through anaphase and cytokinesis in the presence of 1 µg/ml LatA after 3 d of anillin RNAi. This corresponds to Fig. 2 G. Video 9 shows a cell expressing anillin-GFP progressing through anaphase in the presence of 1 µg/ml LatA after 6 d of Septin^{Pnut} RNAi. This corresponds to Fig. 3 D. Video 10 shows a cell expressing anillin-GFP and cherry-tubulin progressing through anaphase in the presence of 1 µg/ml LatA and corresponds to Fig. 4 C. Online supplemental material is available at http://www.jcb.org/cgi/content/full/jcb.200709005/DC1.

We thank members of the O'Farrell laboratory, A. Echard, A. Paoletti, D. Toczyski, and R. Vale, for discussions and C. Sheppard for comments on the manuscript.

This research was supported by a postdoctoral fellowship from Susan G. Komen for the Cure (to G. Hickson), by a Special Fellowship from the Leukemia & Lymphoma Society (to G. Hickson), and by National Institutes of Health grants GM37193 and GM60988 (to P. O'Farrell).

Note added in proof. While this paper was in final review, two independent studies were published demonstrating direct interactions between human anillin and Rho (Piekny and Glotzer, 2008) and between *D. melanogaster* anillin and the MT-bound RhoGAP, RacGAP50C (Gregory et al., 2008). These studies complement our findings of the Rho-dependent control of anillin and the association of anillin with MTs.

Submitted: 4 September 2007
Accepted: 20 December 2007

References

Bement, W.M., H.A. Benink, and G. von Dassow. 2005. A microtubule-dependent zone of active RhoA during cleavage plane specification. *J. Cell Biol.* 170:91–101.

Cao, L.G., and Y.L. Wang. 1990. Mechanism of the formation of contractile ring in dividing cultured animal cells. II. Cortical movement of microinjected actin filaments. *J. Cell Biol.* 111:1905–1911.

Castrillon, D.H., and S.A. Wasserman. 1994. Diaphanous is required for cytokinesis in *Drosophila* and shares domains of similarity with the products of the limb deformity gene. *Development.* 120:3367–3377.

Dean, S.O., and J.A. Spudich. 2006. Rho kinase's role in myosin recruitment to the equatorial cortex of mitotic *Drosophila* S2 cells is for myosin regulatory light chain phosphorylation. *PLoS ONE.* 1:e131.

Dean, S.O., S.L. Rogers, N. Stuurman, R.D. Vale, and J.A. Spudich. 2005. Distinct pathways control recruitment and maintenance of myosin II at the cleavage furrow during cytokinesis. *Proc. Natl. Acad. Sci. USA.* 102:13473–13478.

DeBiasio, R.L., G.M. LaRocca, P.L. Post, and D.L. Taylor. 1996. Myosin II transport, organization, and phosphorylation: evidence for cortical flow/solation-contraction coupling during cytokinesis and cell locomotion. *Mol. Biol. Cell.* 7:1259–1282.

Echard, A., G.R. Hickson, E. Foley, and P.H. O'Farrell. 2004. Terminal cytokinesis events uncovered after an RNAi screen. *Curr. Biol.* 14:1685–1693.

Eggert, U.S., T.J. Mitchison, and C.M. Field. 2006. Animal cytokinesis: from parts list to mechanisms. *Annu. Rev. Biochem.* 75:543–566.

Field, C.M., and B.M. Alberts. 1995. Anillin, a contractile ring protein that cycles from the nucleus to the cell cortex. *J. Cell Biol.* 131:165–178.

Field, C.M., M. Coughlin, S. Doberstein, T. Marty, and W. Sullivan. 2005. Characterization of anillin mutants reveals essential roles in septin localization and plasma membrane integrity. *Development.* 132:2849–2860.

Fishkind, D.J., J.D. Silverman, and Y.L. Wang. 1996. Function of spindle microtubules in directing cortical movement and actin filament organization in dividing cultured cells. *J. Cell Sci.* 109:2041–2051.

Glotzer, M. 2005. The molecular requirements for cytokinesis. *Science.* 307:1735–1739.

Gregory, S.L., S. Ebrahimi, J. Milverton, W.H. Jones, A. Bejsovec, and R. Saint. 2008. Cell division requires a direct link between microtubule-bound RacGAP and Anillin in the contractile ring. *Curr. Biol.* 18:25–29. doi:10.1016/j.cub.2007.11.050.

Guha, M., M. Zhou, and Y.L. Wang. 2005. Cortical actin turnover during cytokinesis requires myosin II. *Curr. Biol.* 15:732–736.

Hickson, G.R., A. Echard, and P.H. O'Farrell. 2006. Rho-kinase controls cell shape changes during cytokinesis. *Curr. Biol.* 16:359–370.

Kamijo, K., N. Ohara, M. Abe, T. Uchimura, H. Hosoya, J.S. Lee, and T. Miki. 2006. Dissecting the role of Rho-mediated signaling in contractile ring formation. *Mol. Biol. Cell.* 17:43–55.

Karess, R.E., X.J. Chang, K.A. Edwards, S. Kulkarni, I. Aguilera, and D.P. Kiehart. 1991. The regulatory light chain of nonmuscle myosin is encoded by spaghetti-squash, a gene required for cytokinesis in *Drosophila*. *Cell.* 65:1177–1189.

Kinoshita, M., C.M. Field, M.L. Coughlin, A.F. Straight, and T.J. Mitchison. 2002. Self- and actin-templated assembly of Mammalian septins. *Dev. Cell.* 3:791–802.

Koppel, D.E., J.M. Oliver, and R.D. Berlin. 1982. Surface functions during mitosis. III. Quantitative analysis of ligand-receptor movement into the cleavage furrow: diffusion vs. flow. *J. Cell Biol.* 93:950–960.

Logarinho, E., H. Bousbaa, J.M. Dias, C. Lopes, I. Amorim, A. Antunes-Martins, and C.E. Sunkel. 2004. Different spindle checkpoint proteins monitor microtubule attachment and tension at kinetochores in *Drosophila* cells. *J. Cell Sci.* 117:1757–1771.

Maddox, A.S., B. Habermann, A. Desai, and K. Oegema. 2005. Distinct roles for two *C. elegans* anillins in the gonad and early embryo. *Development.* 132:2837–2848.

Maddox, A.S., L. Lewellyn, A. Desai, and K. Oegema. 2007. Anillin and the septins promote asymmetric ingression of the cytokinetic furrow. *Dev. Cell.* 12:827–835.

Matsumura, F. 2005. Regulation of myosin II during cytokinesis in higher eukaryotes. *Trends Cell Biol.* 15:371–377.

Murthy, K., and P. Wadsworth. 2005. Myosin II-dependent localization and dynamics of F-actin during cytokinesis. *Curr. Biol.* 15:724–731.

Neufeld, T.P., and G.M. Rubin. 1994. The *Drosophila* peanut gene is required for cytokinesis and encodes a protein similar to yeast putative bud neck filament proteins. *Cell.* 77:371–379.

Oegema, K., M.S. Savoian, T.J. Mitchison, and C.M. Field. 2000. Functional analysis of a human homologue of the *Drosophila* actin binding protein anillin suggests a role in cytokinesis. *J. Cell Biol.* 150:539–552.

Paoletti, A., and F. Chang. 2005. Anillins and mid proteins: organizers of the contractile ring during cytokinesis. *In* Signal Transduction of Cell Division. T. Miki, editor. Research Signpost, Kerala, India. 39–51.

Piekny, A., M. Werner, and M. Glotzer. 2005. Cytokinesis: welcome to the Rho zone. *Trends Cell Biol.* 15:651–658.

Piekny, A.J., and M. Glotzer. 2008. Anillin is a scaffold protein that links RhoA, actin and myosin during cytokinesis. *Curr. Biol.* 18:30–36. doi:10.1016/j.cub.2007.11.068.

Prokopenko, S.N., A. Brumby, L. O'Keefe, L. Prior, Y. He, R. Saint, and H.J. Bellen. 1999. A putative exchange factor for Rho1 GTPase is required for initiation of cytokinesis in *Drosophila*. *Genes Dev.* 13:2301–2314.

Rogers, S.L., U. Wiedemann, U. Hacker, C. Turck, and R.D. Vale. 2004. *Drosophila* RhoGEF2 associates with microtubule plus ends in an EB1-dependent manner. *Curr. Biol.* 14:1827–1833.

Schmidt, K., and B.J. Nichols. 2004. Functional interdependence between septin and actin cytoskeleton. *BMC Cell Biol.* 5:43.

Schroeder, T.E. 1972. The contractile ring. II. Determining its brief existence, volumetric changes, and vital role in cleaving *Arbacia* eggs. *J. Cell Biol.* 53:419–434.

Sisson, J.C., C. Field, R. Ventura, A. Royou, and W. Sullivan. 2000. Lava lamp, a novel peripheral Golgi protein, is required for *Drosophila melanogaster* cellularization. *J. Cell Biol.* 151:905–918.

Somers, W.G., and R. Saint. 2003. A RhoGEF and Rho family GTPase-activating protein complex links the contractile ring to cortical microtubules at the onset of cytokinesis. *Dev. Cell.* 4:29–39.

Somma, M.P., B. Fasulo, G. Cenci, E. Cundari, and M. Gatti. 2002. Molecular dissection of cytokinesis by RNA interference in *Drosophila* cultured cells. *Mol. Biol. Cell.* 13:2448–2460.

Straight, A.F., A. Cheung, J. Limouze, I. Chen, N.J. Westwood, J.R. Sellers, and T.J. Mitchison. 2003. Dissecting temporal and spatial control of cytokinesis with a myosin II Inhibitor. *Science.* 299:1743–1747.

Straight, A.F., C.M. Field, and T.J. Mitchison. 2005. Anillin binds nonmuscle myosin II and regulates the contractile ring. *Mol. Biol. Cell.* 16:193–201.

Suzuki, C., Y. Daigo, N. Ishikawa, T. Kato, S. Hayama, T. Ito, E. Tsuchiya, and Y. Nakamura. 2005. ANLN plays a critical role in human lung carcinogenesis through the activation of RHOA and by involvement in the phosphoinositide 3-kinase/AKT pathway. *Cancer Res.* 65:11314–11325.

Wang, Y.L., J.D. Silverman, and L.G. Cao. 1994. Single particle tracking of surface receptor movement during cell division. *J. Cell Biol.* 127:963–971.

Wu, J.Q., V. Sirotkin, D.R. Kovar, M. Lord, C.C. Beltzner, J.R. Kuhn, and T.D. Pollard. 2006. Assembly of the cytokinetic contractile ring from a broad band of nodes in fission yeast. *J. Cell Biol.* 174:391–402.

Yuce, O., A. Piekny, and M. Glotzer. 2005. An ECT2–centralspindlin complex regulates the localization and function of RhoA. *J. Cell Biol.* 170:571–582.

Zhao, W.M., and G. Fang. 2005. Anillin is a substrate of anaphase-promoting complex/cyclosome (APC/C) that controls spatial contractility of myosin during late cytokinesis. *J. Biol. Chem.* 280:33516–33524.